Mathematical Models and Methods in Applied Sciences

Mortaring the two-dimensional edge finite elements for the discretization of some electromagnetic models*

Adnène BEN ABDALLAH

Applications Scientifiques pour le Calcul Intensif, UPR 9069 CNRS, Bât. 506, Université Paris Sud, 91405 Orsay, France. adnene@asci.fr

Faker BEN BELGACEM

Mathématiques pour l'Industrie et la Physique, UMR 5640 CNRS, Univ. Paul Sabatier, 118 route de Narbonne, 31062 Toulouse Cedex 04, France. belgacem@mip-tlse.fr

Yvon MADAY

Laboratoire J.-L. Lions, UMR 7583 CNRS, Univ. Pierre et Marie Curie, 4 place Jussieu, 75252 Paris cedex 05, France. maday@ann.jussieu.fr

Francesca RAPETTI

Laboratoire J.-A. Dieudonné, UMR 6621 CNRS, Univ. Nice et Sophia-Antipolis, Parc Valrose, 06108 Nice cedex 02, France. frapetti@math.unice.fr

We describe the *mortar element method* for the two-dimensional edge finite elements of class $H(\mathrm{curl})$. These finite elements are currently used for the discretization of various models coming from the Maxwell equations and using them in a mortar framework has several interesting applications in the electromagnetic and electrotechnical domains. We develop some technical tools necessary to perform the numerical analysis of this approach. Then, we prove some optimal approximation results and we illustrate the theory by some numerical experiences.

Keywords: edge finite elements, non-matching grids, mortar element method

1. Introduction

Domain decomposition techniques have become a standard way to increase the size of the problems that can be treated through numerical simulation. These techniques

*The authors recall that, despite its late publication, this paper is the starting step toward the application of the mortar element method to electromagnetism.

allow to use efficiently the parallel potentiality of computers and to design robust iterative solvers to accelerate the access to the numerical (approximated) solution.

When dealing with elliptic or parabolic problems, in order to increase even more the flexibility of the domain decomposition approach, the *mortar element method* [19,10] allows to use, in each sub-domain of the decomposition, the proper discretization (of finite element, spectral, finite volume or of wavelet type) well suited to the local (related to the sub-domain) solution behavior and geometrical features. The resulting approximation is optimal in terms of error estimates and convergence rates since the local discretization parameters can be chosen independently over each sub-domain in such a way that each local contribution to the error is balanced. This discretization parameter can either be designed *a priori* or *a posteriori* [42,18] in a suitable way.

The mortar element method has received in the last decade a lot of attention and it is currently used in many area of the numerical simulation such as, for example, for the spectral approximation of Navier Stokes equations (in the primal variables formulation [6,12], and in the ψ or (ψ, ω) formulation [8]), for the finite element approximation of Navier Stokes equations (in the primal variables formulation [3,11]), for the finite element approach of elasticity [37,36]. This method allows also to couple different discretizations, spectral and finite elements [30,10], and more recently finite elements and wavelets [20]. In the area of solution algorithms, many ideas that "work" on standard discretizations have been extended to the mortar framework (iterative sub-structuring [2,1], multigrid [24]).

The mortar element method can be cast in a hybrid framework [9] and, in this case, it has an alternative that can be found in the more recent three field method [5,25]. In order to enlarge even more the domain of application of the mortar element approach, some attempts have been recently realized to extend it to different kind of partial differential problems such as variational inequalities for the modeling of unilateral contacts. We refer to [14,34] where optimal convergence results are proven.

Among the domains that are not currently covered[†], we can quote the electromagnetic wave propagation field and what involves the full set of Maxwell's equations. As far as we know, currently very few efficient solvers exist using domain decomposition, and among them we refer to [7] in the 3D conforming case, where the matching constraints are expressed using Lagrange multipliers[41]. The mortar approach seems to be naturally fitted to that case and bring about all the advantages that have been quoted before (to which can also be added the sliding mesh method [6,27] to approximate eddy currents in turning machines or the potential inter-processor communication saving [15]). According to the local dielectric permittivity ε and to

[†] It was the real situation at the time (1997) when this work was achieved in its old version. Since then, some substantial advances were realized on this topic, we refer, e.g., to [40,26,21].

the magnetic permeability μ this will enable to consider more or less refined grids within each region.

Some functional notations — Let Ω be a bounded Lipschitz domain in $\mathbb{R}^2$; $L^2(\Omega)$ denotes the classical Lebesgue space of square integrable functions, endowed with the norm associated to the inner product

$$(\varphi, \psi) = \int_\Omega \varphi(\boldsymbol{x})\psi(\boldsymbol{x}).$$

We also use the Sobolev space $H^m(\Omega), m \geq 1$, provided with the norm

$$\|\psi\|_{H^m(\Omega)} = \Big(\sum_{0\leq|\nu|\leq m} \|\partial^\nu \psi\|^2_{L^2(\Omega)} \Big)^{\frac{1}{2}},$$

where $\nu = (\nu_1, \nu_2)$ is a multi-index of $\mathbb{N}^2$ of length $|\nu| = \nu_1 + \nu_2$ and ∂^ν stands for $\partial^{\nu_1}_{x_1}\partial^{\nu_2}_{x_2}$. The fractional Sobolev space $H^\tau(\Omega), \tau \in \mathbb{R}_+ \setminus \mathbb{N}$, can be specified by the norm (see [4], [33])

$$\|\psi\|_{H^\tau(\Omega)} = \Big(\|\psi\|^2_{H^m(\Omega)} + \sum_{|\nu|=m} \int_\Omega \int_\Omega \frac{(\partial^\nu \psi(\boldsymbol{x}) - \partial^\nu \psi(\boldsymbol{y}))^2}{|\boldsymbol{x} - \boldsymbol{y}|^{2+2\theta}}\, d\boldsymbol{x}\, d\boldsymbol{y} \Big)^{\frac{1}{2}},$$

where $\tau = m + \theta$, with m the integer part of τ and $\theta \in]0, 1[$ its decimal part. On a portion Γ of the boundary $\partial\Omega$, the space $H^{\frac{1}{2}}(\Gamma)$ is defined to be the set of the traces over Γ of all the functions of $H^1(\Omega)$ and $H^{-\frac{1}{2}}(\Gamma)$ is its dual space. The duality pairing between both spaces is denoted by $\langle \cdot, \cdot \rangle_{\frac{1}{2},\Gamma}$. The space $H^{\frac{1}{2}}_{00}(\Gamma)$ consists of those elements $v \in H^{\frac{1}{2}}(\Gamma)$ whose trivial extension $\tilde{v}$ of v by zero to all $\partial\Omega$ belongs to $H^{\frac{1}{2}}(\partial\Omega)$. Endowed with the image norm $||v||_{H^{\frac{1}{2}}_{00}(\Gamma)} = ||\tilde{v}||_{\frac{1}{2},\partial\Omega}$, the space $H^{\frac{1}{2}}_{00}(\Gamma)$ is strictly embedded in $H^{\frac{1}{2}}(\Gamma)$ and its dual space is denoted by $H^{-\frac{1}{2}}_{00}(\Gamma)$.

2. The continuous problem setting

We are interested in the full Maxwell equations modeling the propagation of an electromagnetic wave through a medium contained in a Lipschitz domain $\underline{\Omega}$ of $\mathbb{R}^3$ with outward normal $\underline{\boldsymbol{n}}$ and tangent vector $\underline{\boldsymbol{t}}$. In the formulation for the wave propagation, the electric and magnetic fields are solutions of an equation of the following form

$$\frac{\partial^2(\tilde{\alpha}\,\underline{\boldsymbol{u}})}{\partial t^2} + \mathbf{curl}\,(\tilde{\beta}\,\mathbf{curl}\,\underline{\boldsymbol{u}}) = \tilde{\boldsymbol{f}}_j \qquad \text{in } \underline{\Omega} \times [0, T] \tag{2.1}$$

with $T > 0$ and **curl** the three-dimensional curl operator. Here, $\underline{\boldsymbol{u}}$ denotes the magnetic $\underline{\boldsymbol{h}}$ or the electric $\underline{\boldsymbol{e}}$ three-dimensional vector field, $\tilde{\alpha}$ and $\tilde{\beta}$ depend on the electric permettivity ε as well as on the magnetic permeability μ and the right-hand side $\tilde{\boldsymbol{f}}_j$ depends, via a spatial or temporal operator, on the current density vector $\underline{\boldsymbol{j}}$.

To complete these equations we need to impose boundary conditions on $\partial\underline{\Omega}\times[0,T]$ and initial conditions on $\underline{\Omega}\times\{0\}$. Let $\underline{\boldsymbol{g}}_D$, $\underline{\boldsymbol{g}}_N$, $\underline{\boldsymbol{H}}$ and $\underline{\boldsymbol{E}}$ be four known vector functions. The boundary $\partial\underline{\Omega}$ is in general split up into three portions: a Dirichlet boundary $\underline{\Gamma}_D$ of positive measure on which

$$\underline{\boldsymbol{u}}\times\underline{\boldsymbol{n}}=\underline{\boldsymbol{g}}_D,$$

a Neumann boundary $\underline{\Gamma}_N$ where

$$\mathbf{curl}\,\underline{\boldsymbol{u}}\times\underline{\boldsymbol{n}}=\underline{\boldsymbol{g}}_N,$$

and an artificial transparent boundary $\underline{\Gamma}_A$ where we prescribe, e.g., the Silver-Muller first order absorbing boundary conditions, they have to be descriminated for the magnetic $\underline{\boldsymbol{h}}$ and electric $\underline{\boldsymbol{e}}$ vector fields,

$$\begin{aligned}\varepsilon^{-1}(\mathbf{curl}\,\underline{\boldsymbol{h}}\times\underline{\boldsymbol{n}}-\underline{\boldsymbol{j}}\times\underline{\boldsymbol{n}})-\sqrt{\frac{\mu}{\varepsilon}}(\frac{\partial\underline{\boldsymbol{h}}}{\partial t}\times\underline{\boldsymbol{n}})\times\underline{\boldsymbol{n}} &= \underline{\boldsymbol{H}},\\ \sqrt{\frac{\mu}{\varepsilon}}\mathbf{curl}\,\underline{\boldsymbol{e}}\times\underline{\boldsymbol{n}}-\mu(\frac{\partial\underline{\boldsymbol{e}}}{\partial t}\times\underline{\boldsymbol{n}})\times\underline{\boldsymbol{n}} &= \underline{\boldsymbol{E}},\end{aligned}$$

The practical role of such an absorbing condition is to allow for a truncation of an unlimited propagation domain to make it bounded and then accessible to numerical simulations. The initial conditions are $\underline{\boldsymbol{e}}_0$ and $\underline{\boldsymbol{h}}_0$ with div $(\mu\,\underline{\boldsymbol{h}}_0)=0$.

In many applications, the domain $\underline{\Omega}$ is an infinite homogeneous cylinder (in the z-direction we have $\underline{\Omega}=\Omega\times\mathbb{R}_z$) and Ω is the cross-section with the boundary partition $\underline{\Gamma}_D=\Gamma_D\times\mathbb{R}_z$, $\underline{\Gamma}_N=\Gamma_N\times\mathbb{R}_z$ and $\underline{\Gamma}_A=\Gamma_A\times\mathbb{R}_z$. We may then be interested in solutions that are invariant through translations along the z axis, thus having the structure $\underline{\boldsymbol{h}}=\underline{\boldsymbol{h}}(x,y)$ or $\underline{\boldsymbol{e}}=\underline{\boldsymbol{e}}(x,y)$ where the point $\boldsymbol{x}=(x,y)$ is a generic point in the cross section Ω. This is the case, for instance, when we compute an electromagnetic wave, solution of (2.1)) that has no magnetic component in the propagating (z-) direction and referred to as a transverse magnetic (TM) wave. Then, the only pertinent fields to compute are the transverse component $\boldsymbol{h}$ of $\underline{\boldsymbol{h}}$ that may be characterized as a two-dimensional field which is solution of a reduced traveling wave equation similar to (2.1) (with the necessary adaptation of the definition of the scalar curl operator) and the component e_z of $\underline{\boldsymbol{e}}$ verifying a scalar wave equation. The other important class of electromagnetic waves are the transverse electric (TE) ones which have no electric component in the z-direction. The two-dimensional field $\underline{\boldsymbol{e}}=(e_x,e_y)$ is then solution of equations similar to (2.1), with the necessary modifications related to 2D (see [35]) and h_z is solution of a scalar wave equation. In the continuous setting both equations are equivalent, i.e., solving $\boldsymbol{e}$ allows to construct h_z without no further calculations and vice-versa. However, as it is well known, when approximating h_z by standard Lagrangian finite elements spurious modes may occur and the physical solution would not be obtained (see [35,31]). The most popular remedy is to resort to edge elements to approximate the

wave equation on $\boldsymbol{e}$, known to provide satisfactory results.

Realizing the numerical analysis of any space/time discretization of the two-dimensional transverse electric equation necessarily requires to look at the ability of the space discretization method to approximate the following boundary value problem

$$\begin{aligned} \alpha \boldsymbol{e} + \mathbf{curl}\,(\beta \,\mathrm{curl}\,\boldsymbol{e}) &= \boldsymbol{f} \qquad \text{in } \Omega, && (2.2)\\ \boldsymbol{e}\cdot\boldsymbol{t} &= 0 \qquad \text{on } \Gamma_D, && (2.3)\\ \beta(\mathrm{curl}\,\boldsymbol{e}) &= j \qquad \text{on } \Gamma_N, && (2.4)\\ \beta(\mathrm{curl}\,\boldsymbol{e}) - \gamma(\boldsymbol{e}\cdot\boldsymbol{t}) &= E \qquad \text{on } \Gamma_A, && (2.5) \end{aligned}$$

for some parameters α, $\beta, \gamma > 0$ and Ω a bounded polygonal domain in $\mathbb{R}^2$. Here, $\boldsymbol{n}$ is the outward unit normal to the cross-section Ω, $\boldsymbol{t}$ is the unit tangential vector to $\partial\Omega$ and

$$\mathbf{curl}\, v = \begin{pmatrix} \partial_y v \\ -\partial_x v \end{pmatrix}, \qquad \mathrm{curl}\,\boldsymbol{v} = \partial_y v_x - \partial_x v_y\,.$$

We shall, henceforth, focus our attention on the study of this problem. The basics of the extension to the three-dimensional case are presented in [13]. As the nature of the boundary conditions has no particular effects on the definition and the analysis of the discrete method, for the sake of simplicity, we shall consider homogeneous Dirichlet boundary conditions only, i.e.,

$$\boldsymbol{e}\cdot\boldsymbol{t} = 0 \qquad \text{on } \partial\Omega. \tag{2.6}$$

The appropriate functional framework for the analysis of problem (2.2)-(2.6) is the space $H(\mathrm{curl}\,,\Omega)$, defined by

$$H(\mathrm{curl}\,,\Omega) = \Big\{ \boldsymbol{v} \in L^2(\Omega)^2; \quad \mathrm{curl}\,\boldsymbol{v} \in L^2(\Omega) \Big\},$$

that, equipped with the graph norm

$$\|\boldsymbol{v}\|_{H(\mathrm{curl}\,,\Omega)} = \Big(\|\boldsymbol{v}\|^2_{L^2(\Omega)^2} + \|\mathrm{curl}\,\boldsymbol{v}\|^2_{L^2(\Omega)} \Big)^{\frac{1}{2}},$$

is of Hilbert type. It is well known that the tangential component operator $\boldsymbol{v} \mapsto (\boldsymbol{v}\cdot\boldsymbol{t})_{|\partial\Omega}$ maps continuously $H(\mathrm{curl},\Omega)$ onto $H^{-\frac{1}{2}}(\partial\Omega)$ (see [32], [29]). The kernel of this operator, denoted in the literature by $H_0(\mathrm{curl},\Omega)$, is thus a closed subset of $H(\mathrm{curl}\,,\Omega)$ and, equipped with the norm $\|\cdot\|_{H(\mathrm{curl}\,,\Omega)}$, is a Hilbert space. We denote it by $\boldsymbol{X}^\Omega$,

$$\boldsymbol{X}^\Omega = \Big\{ \boldsymbol{v} \in H(\mathrm{curl}\,,\Omega); \quad (\boldsymbol{v}\cdot\boldsymbol{t})_{|\partial\Omega} = 0 \Big\},$$

and its norm by $\|\cdot\|_{\boldsymbol{X}^\Omega}$. In the following, for all integrals, we omit to specify the integration variable where possible and not misleading. The weak form of problem (2.2)–(2.6) reads as follows.

Find $\boldsymbol{e} \in \boldsymbol{X}^\Omega$ *such that*

$$\int_\Omega \alpha\, \boldsymbol{e}\cdot\boldsymbol{w} \;+\int_\Omega \beta\,(\mathrm{curl}\,\boldsymbol{e})(\mathrm{curl}\,\boldsymbol{w}) \;=\int_\Omega \boldsymbol{f}\cdot\boldsymbol{w}\;, \qquad \forall \boldsymbol{w}\in \boldsymbol{X}^\Omega. \tag{2.7}$$

The bilinear form defined by the left-hand side of (2.7) is continuous, symmetric and coercive over $\boldsymbol{X}^\Omega$ with an ellipticity constant equal to $\min(\alpha,\beta)$ and, hence, problem (2.7) has a unique solution, by the Lax-Milgram Lemma.

The outline of the remainder of this paper is as follows. Section 3 is dedicated to the description of the mortar element method applied to problem (2.7). The finite elements used here are those of class $H(\mathrm{curl})$ introduced by J.-C. Nédélec in [39] commonly known as the second family of edge finite elements. We then perform a complete study of the discrete problem, i.e., existence, uniqueness of a solution and error analysis. Section 4 is a validation of the method with some numerical examples. The reader interested in the application of the mortar edge finite element approach to the electrotechnical models (eddy currents) is recommended to look at [40] for some relevent examples.

3. The mortar edge finite element framework

The domain decomposition algorithm proceeds by breaking up the domain Ω into K non-overlapping sub-domains (assumed to be provided with a boundary that is at least Lipschitz connected),

$$\overline{\Omega} = \bigcup_{k=1}^{K} \overline{\Omega}_k \quad \text{ with } \Omega_k\cap\Omega_\ell=\emptyset, \quad \text{ if } k\neq\ell.$$

With each sub-domain Ω_k we associate a regular triangulation $\mathscr{T}_k$ composed of triangles. We note that it is possible to extend what follows to triangulations $\mathscr{T}_k$ involving either triangles or quadrangles or both of them. The extension to more general situations does not give rise to any particular difficulty. Besides we assume, to avoid the technicalities of the curved finite elements, that each sub-domain Ω_k (and thus Ω) is a polygon and also that each edge of Ω_k meeting the boundary $\partial\Omega$ is entirely contained in it and we set

$$\overline{\Omega}_k = \bigcup_{\kappa\in\mathscr{T}_k} \overline{\kappa}\,.$$

We denote by $\Gamma_{k,i}$, $1\le i\le I(k)$ the (macro) edges of Ω_k, their union is $\partial\Omega_k$ and the outward normal unit vector is $\boldsymbol{n}_k$ while the tangential one is $\boldsymbol{t}_k$. Each such a face inherits a triangulation from Ω_k that is denoted by $\mathscr{T}_{k,i}$. Note that, since

the triangulations on two adjacent sub-domains are independent, the interface is provided with two different and independent discretizations.

For any integer $q \geq 0$, $\mathcal{P}_q$ stands for the space of polynomials on $\mathbb{R}$ with global degree $\leq q$ while $\tilde{\mathcal{P}}_q$ is the subspace of homogeneous polynomials on $\mathbb{R}$ with degree q; we introduce the space

$$\mathscr{D}_q(\kappa) = \mathcal{P}_{q-1}(\kappa)^2 + \tilde{\mathcal{P}}_{q-1}(\kappa)\boldsymbol{x}.$$

The dimension of $\mathscr{D}_q(\kappa)$ is $q(q+2)$. The finite element space we need to use locally is that developed in [39] and, for any k, is given by

$$\boldsymbol{X}_h^{\Omega_k} = \Big\{\boldsymbol{v}_h \in H(\mathrm{curl}\,,\Omega_k), \qquad \forall \kappa \in \mathscr{T}_k, \qquad \boldsymbol{v}_{h|\kappa} \in \mathcal{P}_q(\kappa)^2\Big\}.$$

In order to explicit the degrees of freedom of the discrete space $\boldsymbol{X}_h^{\Omega_k}$, following [39], we denote by $(f_j^\kappa)_{1\leq j\leq 3}$ the three edges of each triangle κ and denote by $\boldsymbol{t}_j^\kappa, 1 \leq j \leq 3$ the tangent unit vectors to these edges (f_j^κ). The degrees of freedom associated with $\boldsymbol{X}_h^{\Omega_k}$ are then

$$\int_{f_j^\kappa} (\boldsymbol{v}_h \cdot \boldsymbol{t}_j^\kappa)\, p \qquad \forall\, p \in \mathcal{P}_q(f_j^\kappa),\ \forall \kappa \in \mathscr{T}_k\,,$$

$$\int_\kappa \boldsymbol{v}_h \cdot \boldsymbol{p} \qquad \forall\, \boldsymbol{p} \in \mathscr{D}_{q-1}(\kappa)^2,\ \forall \kappa \in \mathscr{T}_k\,.$$

Their total number is $3(q+1)+(q-1)(q+1) = (q+1)(q+2)$ coincides of course with the dimension of $\mathcal{P}_q(\kappa)^2$. The set of these degrees of freedom allows to determine for any $\boldsymbol{v} \in H(\mathrm{curl}\,,\Omega_k)$ a unique interpolate $i_h^k \boldsymbol{v} \in \boldsymbol{X}_h^{\Omega_k}$ satisfying the following error estimate (see [39]): for any $\boldsymbol{v} \in H^q(\Omega_k)^2$ such that curl $\boldsymbol{v} \in H^q(\Omega_k)$ we have:

$$\|\boldsymbol{v} - i_h^k \boldsymbol{v}\|_{\boldsymbol{X}^{\Omega_k}} \leq C h^q \big(\|\boldsymbol{v}\|_{H^q(\Omega_k)^2} + \|\mathrm{curl}\,\boldsymbol{v}\|_{H^q(\Omega_k)}\big). \tag{3.8}$$

Over any edge $\Gamma_{k,i}$ of Ω_k the tangential traces of the functions of $\boldsymbol{X}_h^{\Omega^k}$ consist in discontinuous piece-wise polynomial functions of degree $\leq q$, so that, denoting by $W_h(\Gamma_{k,i})$ the space

$$W_h(\Gamma_{k,i}) = \Big\{\psi_h = \boldsymbol{v}_h \cdot \boldsymbol{t}_{|\Gamma_{k,i}}, \qquad \boldsymbol{v}_h \in \boldsymbol{X}_h^{\Omega_k}\Big\}$$

we have that

$$W_h(\Gamma_{k,i}) = \Big\{\psi_h \in L^2(\Gamma_{k,i}), \quad \forall f \in \mathscr{T}_{k,i}, \quad \psi_{h|f} \in \mathcal{P}_q(f)\Big\}.$$

The description of the topological features of the mortar element method starts by introducing the skeleton

$$\mathcal{S} = \bigcup_{k=1}^{K} \partial\Omega_k = \bigcup_{k=1}^{K} \bigcup_{i=1}^{I(k)} \Gamma_{k,i}.$$

Among the many possible decompositions of $\mathcal{S}$ we choose a splitting of $\mathcal{S}$ as the disjoint union of some edges $\Gamma_{k,i}$, which are called *mortars*. In detail, we set

$$\mathcal{S} = \bigcup_{m=1}^{m^*} \gamma_m, \quad \text{with } \gamma_m \cap \gamma_{m'} = \emptyset, \quad \text{if } m \neq m',$$

and any mortar γ_m is an entire edge of at least one sub-domain $\Omega_{k(m)}$, i.e.,

$$\forall m, 1 \leq m \leq m^*, \qquad \exists (k(m), i(m)), \quad \gamma_m = \Gamma_{k(m),i(m)}.$$

We note that this partition is not in general unique (see Figure 1 for an example of different choices of the mortars family).

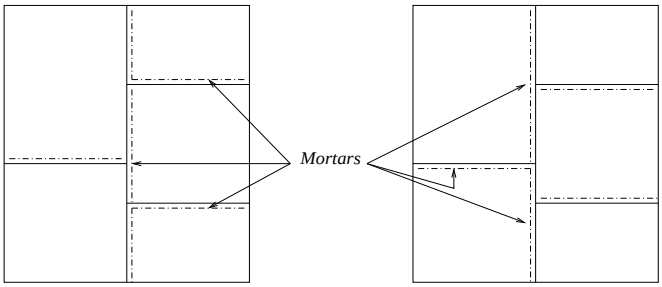

Figure 1: Multiple choices of the mortars family are possible.

The mortar element method allows to work with discrete functions over Ω with discontinuous tangential traces across the interfaces, thus these functions do not belong to $\boldsymbol{X}^{\Omega}$. Instead, they satisfy some integral matching conditions that glue them across the interfaces. In order to express these constraints we need some suitable functions belonging to the space

$$W_h^{\mathcal{S}} = \Big\{ \varphi_h \in L^2(\mathcal{S}), \quad \forall m,\ 1 \leq m \leq m^*,\ \varphi_{h|\gamma_m} \in W_h(\Gamma_{k(m),i(m)}), \quad \varphi_{h|\partial\Omega} = 0 \Big\},$$

called the mortar space and the discrete space is then given by

$$\begin{aligned} \boldsymbol{X}_h^{\Omega} = \Big\{ \boldsymbol{v}_h \ \in\ & L^2(\Omega)^2,\ \boldsymbol{v}_h^k = \boldsymbol{v}_{h|\Omega_k} \in \boldsymbol{X}_h^{\Omega_k},\ \ \forall\, k,\ 1 \leq k \leq K, \\ \exists\ & \varphi_h \in W_h^{\mathcal{S}},\ \ \forall\, k,\ 1 \leq k \leq K,\ \ \forall i,\ 1 \leq i \leq I(k), \\ & \int_{\Gamma_{k,i}} \big((\boldsymbol{v}_h^k \cdot \boldsymbol{t}_k)_{|\Gamma_{k,i}} - \varphi_{h|\Gamma_{k,i}} \big) \psi_h \, d\Gamma = 0 \ ,\ \forall\ \psi_h \in W_h(\Gamma_{k,i}) \ \Big\}. \end{aligned} \tag{3.9}$$

It is clear that any vector field $\boldsymbol{v}_h \in \boldsymbol{X}_h^{\Omega}$ is associated with only one mortar function, since it is checked that, $\forall m, 1 \leq m \leq m^*$,

$$\varphi_{h|\gamma_m} = (\boldsymbol{v}_h^{k(m)} \cdot \boldsymbol{t}_{k(m)})_{|\Gamma_{k(m),i(m)}}.$$

Besides, letting $\pi_{k,i}$ be the orthogonal projection operator mapping $L^2(\Gamma_{k,i})$ onto $W_h(\Gamma_{k,i})$, we have that: $\boldsymbol{v}_h$ belongs to $\boldsymbol{X}_h^\Omega$ if and only if there exists $\varphi_h \in W_h^{\mathcal{S}}$ such that, $\forall k, \forall i$,

$$(\boldsymbol{v}_h^k \cdot \boldsymbol{t}_k)_{|\Gamma_{k,i}} = \pi_{k,i}(\varphi_{h|\Gamma_{k,i}}).$$

We recall that $\pi_{k,i}$ satisfies the following error estimate: for any $\varphi \in H^q(\Gamma_{k,i})$,

$$\|\varphi - \pi_{k,i}\varphi\|_{L^2(\Gamma_{k,i})} + h^{-\frac{1}{2}}\|\varphi - \pi_{k,i}\varphi\|_{H^{-\frac{1}{2}}(\Gamma_{k,i})} \leq Ch^q\|\varphi\|_{H^q(\Gamma_{k,i})}. \tag{3.10}$$

This bound on the L^2-norm is classical and that on the $H^{-\frac{1}{2}}$–norm is derived by means of the Aubin-Nitsche duality argument.
The mortar approach being non-Hodge conforming, since $\boldsymbol{X}_h^\Omega \not\subset \boldsymbol{X}^\Omega$, we need to introduce the broken norm of the space $\boldsymbol{X}_*^\Omega = \prod_{k=1}^K \boldsymbol{X}^{\Omega_k}$ defined by

$$\|\boldsymbol{v}\|_{\boldsymbol{X}_*^\Omega} = \Big(\sum_{k=1}^K \|\boldsymbol{v}^k\|^2_{\boldsymbol{X}^{\Omega_k}}\Big)^{\frac{1}{2}}, \qquad \forall \boldsymbol{v} = (\boldsymbol{v}^k)_k \in \boldsymbol{X}_*^\Omega.$$

The discrete problem associated with the variational formulation (2.7) reads:

Find $\boldsymbol{e}_h \in \boldsymbol{X}_h^\Omega$ *such that*

$$\int_\Omega \alpha\, \boldsymbol{e}_h \cdot \boldsymbol{w}_h \; + \sum_{k=1}^K \int_{\Omega_k} \beta\, (\operatorname{curl} \boldsymbol{e}_h^k)(\operatorname{curl} \boldsymbol{w}_h^k) \; = \int_\Omega \boldsymbol{f} \cdot \boldsymbol{w}_h, \qquad \forall \boldsymbol{w}_h \in \boldsymbol{X}_h^\Omega. \tag{3.11}$$

The bilinear form associated to (3.11) is symmetric and elliptic; problem (3.11) has then only one solution in $\boldsymbol{X}_h^\Omega$.

Remark 3.1 *It has to be noticed that the method we propose is in the spirit of the former mortar element method. Indeed, the constraints* (3.9) *involve a space of Lagrange multipliers*[‡] *that is defined as a subspace of the (tangential) traces of the discrete functions over each* Ω_k*. Note also that here this space coincides exactly with the full space of tangential traces in opposition to the former examples (e.g. associated with discretization of* $H^1(\Omega)$*) where a constraint (of zero slope for* $\mathcal{P}_1$*-approximations) is imposed on the two end parts of each interface* $\Gamma_{k,i}$*. The reason lies on the fact that the tangential traces on two adjacent edges of the same subdomain are completely independent. This feature is specific to the two-dimensional case (see* [13,22]*, for the three dimensions).*

4. Numerical analysis

The evaluation of the error $\|\boldsymbol{e} - \boldsymbol{e}_h\|_{\boldsymbol{X}_*^\Omega}$ is based on the Berger-Scott-Strang Lemma commonly known under the second Strang Lemma (see [16], [28]), adapted to our context.

[‡]The equivalent formulation of problem (3.11) as a saddle point problem will be thoroughly studied in a forthcoming work.

Lemma 4.1 *The solutions $\boldsymbol{e}$ and $\boldsymbol{e}_h$ of the exact and discrete problems verify*

$$\|\boldsymbol{e}-\boldsymbol{e}_h\|_{\boldsymbol{X}_*^\Omega} \leq C\Big(\inf_{\boldsymbol{w}_h\in\boldsymbol{X}_h^\Omega}\|\boldsymbol{e}-\boldsymbol{w}_h\|_{\boldsymbol{X}_*^\Omega} + \sup_{\boldsymbol{w}_h\in\boldsymbol{X}_h^\Omega}\frac{1}{\|\boldsymbol{w}_h\|_{\boldsymbol{X}_*^\Omega}}\sum_{k=1}^{K}\langle \boldsymbol{w}_h^k\cdot\boldsymbol{t},(\operatorname{curl}\boldsymbol{e})\rangle_{\frac12,\partial\Omega_k}\Big). \quad (4.12)$$

Note that, the trace of (curl $\boldsymbol{e}$) over $\partial\Omega_k$ belongs to $H^{\frac12}(\partial\Omega_k)$ (because $\boldsymbol{e}\in L^2(\Omega)^2$ and from (2.2) we obtain that $\operatorname{grad}\boldsymbol{e}\in L^2(\Omega)$ and then the duality pairing of the right-hand side makes sense. It results from Lemma 4.1 that the global error is the sum of two contributions: the (classical) best approximation error, represented by the first term in the right-hand side of (4.12), and the consistency error, due to the non-conformity of the approximation and given by the remaining part of (4.12). This last term measures the *variational crime* committed on the discrete solution. Both errors are analyzed separately.

4.1. *The best approximation error*

The goal is to examine how close the discrete space $\boldsymbol{X}_h^\Omega$ is to $\boldsymbol{X}^\Omega$. This study involves some preliminary results related in particular to the stability of some extension operators in finite element spaces of class $H(\operatorname{curl})$ designed on arbitrary regular meshes (we stress on the fact that the quasi uniform regularity of the local discretizations is not required here). Let us denote $W_h(\partial\Omega_k)=\prod_{i=1}^{I(k)}W_h(\Gamma_{k,i})$ for any $k\,(1\leq k\leq K)$.

Theorem 4.2 *The tangential trace operator mapping $\boldsymbol{X}_h^{\Omega_k}$ onto $W_h(\partial\Omega_k)$ has a continuous right inverse $\mathscr{R}_k$, i.e. $\mathscr{R}_k$ is such that $(\mathscr{R}_k\varphi_h)\cdot\boldsymbol{t}_{k|\partial\Omega_k}=\varphi_h$ and the following stability condition holds:*

$$\|\mathscr{R}_k\varphi_h\|_{\boldsymbol{X}^{\Omega_k}}\leq C\|\varphi_h\|_{H^{-\frac12}(\partial\Omega_k)},\qquad \forall\varphi_h\in W_h(\partial\Omega_k).$$

The constant C does not depend on the mesh size h.

The proof of Theorem 4.2 requires some preparation Lemmas. We shall skip over the index k for a while. For any $\varphi\in H^{-\frac12}(\partial\Omega)$, let us consider the decomposition $\varphi=\tilde\varphi+\xi$ with $\tilde\varphi$ a zero-averaged distribution, i.e., $\langle\tilde\varphi,1\rangle_{\frac12,\partial\Omega}=0$, and $\xi=\frac{1}{\operatorname{mes}(\partial\Omega)}\langle\varphi,1\rangle_{\frac12,\partial\Omega}$. We then have the following Lemma.

Lemma 4.3 *There exists a constant $c>0$ such that for any $\varphi\in H^{-\frac12}(\partial\Omega)$, we have*

$$\Big(\|\tilde\varphi\|^2_{H^{-\frac12}(\partial\Omega)}+|\xi|^2\Big)^{\frac12}\leq c\|\varphi\|_{H^{-\frac12}(\partial\Omega)}.$$

Proof: For any $\psi\in H^{\frac12}(\partial\Omega)$ decomposed as $\psi=\tilde\psi+\delta$ with $\delta=\frac{1}{\operatorname{mes}(\partial\Omega)}\int_{\partial\Omega}\psi\,d\Gamma$ (so that $\tilde\psi$ is zero-averaged), the following equality is straightforward

$$\|\psi\|^2_{H^{\frac12}(\partial\Omega)}=\|\tilde\psi\|^2_{H^{\frac12}(\partial\Omega)}+\delta^2\|1\|^2_{L^2(\partial\Omega)}. \quad (4.13)$$

Then, for any φ written as above, $\varphi = \tilde{\varphi} + \xi \in H^{-\frac{1}{2}}(\partial\Omega)$, we have, by duality,

$$\|\tilde{\varphi}\|_{H^{-\frac{1}{2}}(\partial\Omega)} = \sup_{\psi \in H^{\frac{1}{2}}(\partial\Omega)} \frac{\langle \tilde{\varphi}, \psi \rangle_{\frac{1}{2},\partial\Omega}}{\|\psi\|_{H^{\frac{1}{2}}(\partial\Omega)}}.$$

Using the fact that

$$\langle \tilde{\varphi}, \psi \rangle_{\frac{1}{2},\partial\Omega} \;=\; \langle \tilde{\varphi}, \tilde{\psi} \rangle_{\frac{1}{2},\partial\Omega} \;=\; \langle \varphi, \tilde{\psi} \rangle_{\frac{1}{2},\partial\Omega},$$

we deduce via (4.13) that

$$\|\tilde{\varphi}\|_{H^{-\frac{1}{2}}(\partial\Omega)} \leq \|\varphi\|_{H^{-\frac{1}{2}}(\partial\Omega)} \sup_{\psi \in H^{\frac{1}{2}}(\partial\Omega)} \frac{\|\tilde{\psi}\|_{H^{\frac{1}{2}}(\partial\Omega)}}{\|\psi\|_{H^{\frac{1}{2}}(\partial\Omega)}} \leq \|\varphi\|_{H^{-\frac{1}{2}}(\partial\Omega)}.$$

On the other side, arguing in the same way and because of the equality

$$\langle \xi, \psi \rangle_{\frac{1}{2},\partial\Omega} \;=\; \langle \xi, \delta \rangle_{\frac{1}{2},\partial\Omega} \;=\; \langle \varphi, \delta \rangle_{\frac{1}{2},\partial\Omega},$$

we obtain that

$$\|\xi\|_{H^{-\frac{1}{2}}(\partial\Omega)} = |\xi|\, \|1\|_{H^{-\frac{1}{2}}(\partial\Omega)} \leq \|\varphi\|_{H^{-\frac{1}{2}}(\partial\Omega)} \sup_{\psi \in H^{\frac{1}{2}}(\partial\Omega)} \frac{\|\delta\|_{H^{\frac{1}{2}}(\partial\Omega)}}{\|\psi\|_{H^{\frac{1}{2}}(\partial\Omega)}} \leq \|\varphi\|_{H^{-\frac{1}{2}}(\partial\Omega)}.$$

Summing up both inequalities and using (4.13) yields the result. □

Before giving the next Lemma let us denote $(\boldsymbol{c}_i)_{0\leq i\leq I}$ the corners of Ω numbered so that $\boldsymbol{c}_i$ is the common vertex of Γ_i and Γ_{i+1}. Then, we consider the local polar system with origin $\boldsymbol{c}_i$. For any point $\boldsymbol{x}$, the positive real number r_i measures the distance between $\boldsymbol{c}_i$ and $\boldsymbol{x}$ and θ_i is the angle from Γ_i to $(\boldsymbol{c}_i\boldsymbol{x})$ in the trigonometric sense. For any $i, 0 \leq i \leq I$, we define η_i as a truncation function of $\mathscr{D}(\overline{\Omega})$ (the space of indefinitely smooth functions with support contained in $\overline{\Omega}$) which does not depend on θ_i and is such that $\eta_i \equiv 1$ near $\boldsymbol{c}_i$ and $\eta_i \equiv 0$ near all Γ_j for $i \neq j$ and $i \neq j+1$. Besides, the intersection of the supports of η_i and η_j, for $i \neq j$, is empty.

Lemma 4.4 *There exists a function $\chi \in H^3(\Omega)$ such that $\partial_{\boldsymbol{n}}\chi_{|\partial\Omega} = 1$.*

Proof: Let us consider $\eta_* \in \mathscr{D}(\overline{\Omega})$ such that $((\eta_i)_{0\leq i\leq I}, \eta_*)$ is a partition of unity (i.e. $\sum_{i=1}^{I} \eta_i + \eta_* \equiv 1$). It is immediate that for any $i, \eta_{*|\Gamma_i} \in H^{\frac{3}{2}}(\Gamma_i)$ and $(0, \eta_{*|\partial\Omega})$ satisfies the required compatibility conditions at the corners (see [33]) to be the trace of a function $\chi_* \in H^3(\Omega)$, which means that

$$\chi_{*|\partial\Omega} = 0, \qquad \partial_{\boldsymbol{n}}\chi_{*|\partial\Omega} = \eta_*.$$

Then, at the vicinity of any corner $\boldsymbol{c}_i$ we set

$$\chi_i(r_i, \theta_i) = -\eta_i(r_i)\big(\cot(\frac{\omega_i}{2}) r_i \cos(\theta_i) - r_i \sin(\theta_i)\big).$$

This function is the product of η_i by a first degree polynomial and, recalling that $\partial_{\boldsymbol{n}}\chi = r_i^{-1}\partial_\theta\chi_i$, it is easy to check that in particular $\partial_{\boldsymbol{n}}\chi_{i|\partial\Omega} = \eta_i$. Then, summing up over i we obtain that the function

$$\chi = \chi_* + \sum_{i=1}^{I} \chi_i,$$

belongs to $H^3(\Omega)$ and satisfies the desired result. □

We recall also that, when $Y_h^{\Omega_k}$ is the Lagrange finite element space of degree $q+1$ associated with $H^1(\Omega_k)$,

$$Y_h^{\Omega_k} = \Big\{\chi_h \in \mathscr{C}(\overline{\Omega}_k), \qquad \forall \kappa \in \mathscr{T}_k, \qquad \chi_{h|\kappa} \in \mathcal{P}_{q+1}(\kappa)\Big\},$$

the gradient operator ranges $Y_h^{\Omega_k}$ into $\boldsymbol{X}_h^{\Omega_k}$. The space $Y_h^{\partial\Omega_k}$ denotes the range of $Y_h^{\Omega_k}$ by the trace operator.

Let us recall now the following extension Lemma due to [17] that allows to deal with non-quasi-uniform meshes.

Lemma 4.5 *For any k, $1 \le k \le K$, and any $h_k > 0$, the trace operator from $Y_h^{\Omega_k}$ provided with the $H^1(\Omega^k)$-norm onto $Y_h^{\partial\Omega_k}$ provided with the $H^{\frac{1}{2}}(\partial\Omega_k)$-norm, admits a right inverse that is uniformly continuous with respect to h_k*

Proof of Theorem 4.2 : Let φ_h be in $\prod_{i=1}^{I} W_h(\Gamma_i)$ and decomposed as $\varphi_h = \tilde{\varphi}_h + \xi$ with $\int_{\partial\Omega} \tilde{\varphi}_h \, d\Gamma = 0$. The construction of a stable extension of φ_h takes two steps, corresponding to separate extensions of $\tilde{\varphi}_h$ and ξ.
i.– Let us consider $s \mapsto \boldsymbol{x}(s)$ a $\mathscr{C}^1$–piece-wise parameterization of the boundary $\partial\Omega$ where s varies in $[0,\ell]$, ℓ is the length of $\partial\Omega$, $\boldsymbol{x}(0) = \boldsymbol{x}(\ell)$ and

$$\psi_h(\boldsymbol{x}(s')) = \int_0^{s'} \tilde{\varphi}_h(\boldsymbol{x}(s)) \, ,$$

which is a continuous piece-wise polynomial of $Y_h^{\partial\Omega}$. Using Lemma 4.5 it is possible to find $\chi_h \in Y_h^{\Omega}$ such that $\chi_{h|\partial\Omega} = \psi_h$ and

$$\|\chi_h\|_{H^1(\Omega)} \le c\|\psi_h\|_{H^{\frac{1}{2}}(\partial\Omega)} \le c\|\tilde{\varphi}_h\|_{H^{-\frac{1}{2}}(\partial\Omega)}.$$

Next, we define the vector field $\boldsymbol{w} = \operatorname{grad}\chi_h$, it can be readily checked that $\boldsymbol{w}$ is in $\boldsymbol{X}_h^{\Omega}$ with

$$(\boldsymbol{w}_h \cdot \boldsymbol{t})_{|\partial\Omega} = \partial_{\boldsymbol{t}}\chi_h = \partial_{\boldsymbol{t}}\psi_h = \tilde{\varphi}_h.$$

Furthermore $\boldsymbol{w}_h$ satisfies the stability condition

$$\|\boldsymbol{w}_h\|_{\boldsymbol{X}^\Omega} \le \|\operatorname{grad}\chi_h\|_{(L^2(\Omega))^2} \le c\|\tilde{\varphi}\|_{H^{-\frac{1}{2}}(\partial\Omega)}.$$

ii.– For the lifting of the constant ξ, we use the function χ of Lemma 4.4. Then the vector field defined by $\boldsymbol{v} = -\xi \mathbf{curl}\, \chi$ belongs to $(H^{1+\varepsilon}(\Omega))^2$ and its tangential trace $(\boldsymbol{v}\cdot\boldsymbol{t})_{|\partial\Omega}$ coincides with $\xi\partial_{\boldsymbol{n}}\chi = \xi$. Moreover, from the regularity of χ we have

$$\|\boldsymbol{v}\|_{\boldsymbol{X}^\Omega} + \|\boldsymbol{v}\|_{H^{1+\varepsilon}(\Omega)} \leq C|\xi| \leq C\|\xi\|_{H^{-\frac{1}{2}}(\partial\Omega)}.$$

Next, we set $\boldsymbol{v}_h = i_h\boldsymbol{v} \in \boldsymbol{X}_h^\Omega$, we notice immediately that again $\boldsymbol{v}_h \cdot \boldsymbol{t}_{|\partial\Omega} = \xi$ and

$$\begin{aligned}\|\boldsymbol{v}_h\|_{\boldsymbol{X}^\Omega} &\leq \|\boldsymbol{v}_h - \boldsymbol{v}\|_{\boldsymbol{X}^\Omega} + \|\boldsymbol{v}\|_{\boldsymbol{X}^\Omega}\\ &\leq Ch^\varepsilon\|\boldsymbol{v}\|_{H^{1+\varepsilon}(\Omega)} + \|\boldsymbol{v}\|_{\boldsymbol{X}^\Omega}\\ &\leq C|\xi| \leq C\|\xi\|_{H^{-\frac{1}{2}}(\partial\Omega)}.\end{aligned}$$

Thus, taking $\mathscr{R}\varphi_h = \boldsymbol{w}_h + \boldsymbol{v}_h$ and using the previous lemma we achieve the proof. □

The main result of this section deals with the convergence rate of the best approximation error and is provided by the following theorem.

Theorem 4.6 *There exists a constant $C > 0$ such that for any $\boldsymbol{e} \in \boldsymbol{X}^\Omega$ with $\boldsymbol{e}^k = \boldsymbol{e}_{|\Omega_k} \in H^q(\Omega_k)^2$ and* curl $\boldsymbol{e}^k \in H^q(\Omega_k)$*, we have*

$$\inf_{\boldsymbol{v}_h\in\boldsymbol{X}_h^\Omega} \|\boldsymbol{e} - \boldsymbol{v}_h\|_{\boldsymbol{X}_*^\Omega} \leq C\sum_{k=1}^K h_k^q\big(\|\boldsymbol{e}^k\|_{H^q(\Omega_k)^2} + \|\mathrm{curl}\, \boldsymbol{e}^k\|_{H^q(\Omega_k)}\big). \tag{4.14}$$

Proof: It is performed following the same points as in [19]. Indeed, we begin by determining a local approximation $\boldsymbol{w}_h^k \in \boldsymbol{X}_h^{\Omega_k}$ in each sub-domain (it may be taken equal to $i_h^k\boldsymbol{e}_{|\Omega_k}$), that satisfies

$$\sum_{k=1}^K \|\boldsymbol{e}_{|\Omega_k} - \boldsymbol{w}_h^k\|_{\boldsymbol{X}^{\Omega_k}} \leq \sum_{k=1}^K h_k^q\big(\|\boldsymbol{e}^k\|_{H^q(\Omega_k)^2} + \|\mathrm{curl}\, \boldsymbol{e}^k\|_{H^q(\Omega_k)}\big). \tag{4.15}$$

The global function $\boldsymbol{w}_h = (\boldsymbol{w}_h^k)_{1\leq k\leq K}$ does not belong to $\boldsymbol{X}_h^\Omega$ because it does not satisfy the matching constraints across the interfaces. To build $\boldsymbol{e}_h \in \boldsymbol{X}_h^\Omega$ close to $\boldsymbol{e}$ we need to define a mortar function φ_h, that coincides with $(\boldsymbol{w}_h^{k(m)}\cdot\boldsymbol{t})_{k|\Gamma_{k(m),i(m)}}$ over each mortar γ_m. This element belongs to $W_h^{\mathcal{S}}$. Then, within each sub-domain it is necessary to modify the values of $\boldsymbol{w}_h^k$ over the edges $\Gamma_{k,i}$ that are not mortars. Let r_h^k denote the residual function defined on $\partial\Omega_k$, equal to $\pi_{k,i}(\varphi_{h|\Gamma_{k,i}} - \boldsymbol{w}_h^k\cdot\boldsymbol{t}_{k|\Gamma_{k,i}})$ over $\Gamma_{k,i}$ when it is not a mortar and vanishing otherwise. Then, we define the new local approximation by

$$\boldsymbol{e}_h^k = \boldsymbol{w}_h^k + \mathscr{R}_k r_h^k.$$

By construction, $\boldsymbol{e}_h = (\boldsymbol{e}_h^k)_{1\leq k\leq K}$ is in $\boldsymbol{X}_h^\Omega$. Besides, the stability of the extension operators $(\mathscr{R}_k)_k$ and the triangular inequality altogether yield

$$\|\mathscr{R}_k r_h^k\|_{\boldsymbol{X}^{\Omega_k}} \leq C\|r_h^k\|_{H^{-\frac{1}{2}}(\partial\Omega_k)}$$

and then

$$\begin{aligned}\|\mathscr{R}_k r_h^k\|_{\boldsymbol{X}^{\Omega_k}} \;\le\; & C\Big(\sum_{i=1}^{I(k)} \|(\varphi_{h|\Gamma_{k,i}} - \boldsymbol{e}\cdot\boldsymbol{t}_{k|\Gamma_{k,i}}) - \pi_{k,i}(\varphi_{h|\Gamma_{k,i}} - \boldsymbol{e}\cdot\boldsymbol{t}_{k|\Gamma_{k,i}})\|_{H^{-\frac{1}{2}}(\Gamma_{k,j})} \\ & + \sum_{i=1}^{I(k)} \|\boldsymbol{e}\cdot\boldsymbol{t}_{k|\Gamma_{k,i}} - \pi_{k,i}(\boldsymbol{e}\cdot\boldsymbol{t}_{k|\Gamma_{k,i}})\|_{H^{-\frac{1}{2}}(\Gamma_{k,i})} \\ & + \sum_{i=1}^{I(k)} \|\varphi_{h|\Gamma_{k,i}} - \boldsymbol{w}_h^k\cdot\boldsymbol{t}_{k|\Gamma_{k,i}}\|_{H^{-\frac{1}{2}}(\Gamma_{k,i})}\Big).\end{aligned}$$

Making use of the truncation error estimate (3.10) of $\pi_{k,i}$, we obtain

$$\begin{aligned}\|\mathscr{R}_k r_h^k\|_{\boldsymbol{X}^{\Omega_k}} \;\le\; & C\Big(h_k^{\frac{1}{2}}\|\varphi_{h|\partial\Omega_k} - \boldsymbol{e}\cdot\boldsymbol{t}_{k|\partial\Omega_k}\|_{L^2(\partial\Omega_k)} + h_k^q\|\boldsymbol{e}\cdot\boldsymbol{t}_{k|\partial\Omega_k}\|_{H^{q-\frac{1}{2}}(\partial\Omega_k)} \\ & + \sum_{i=1}^{I(k)} \|\varphi_{h|\Gamma_{k,i}} - \boldsymbol{e}\cdot\boldsymbol{t}_{k|\Gamma_{k,i}}\|_{H^{-\frac{1}{2}}(\Gamma_{k,i})} \\ & + \sum_{i=1}^{I(k)} \|\boldsymbol{w}_h^k\cdot\boldsymbol{t}_{k|\Gamma_{k,i}} - \boldsymbol{e}\cdot\boldsymbol{t}_{k|\Gamma_{k,i}}\|_{H^{-\frac{1}{2}}(\Gamma_{k,i})}\Big).\end{aligned}$$

Finally, we sum over k and employ (4.15) together with the trace theorem. By recalling that φ_h is the tangential trace on the mortar γ_m of $\boldsymbol{w}_h^{k(m)}$, we get (4.14).□

4.2. *Consistency error*

Let us turn to the consistency error. An optimal bound of this error is provided in the following Lemma.

Lemma 4.7 *When the solution $\boldsymbol{e}$ of the exact problem satisfies similar regularity assumptions as those of Theorem* 4.6 *and that for $k, 1 \le k \le K$, the data $\boldsymbol{f}^k = \boldsymbol{f}_{|\Omega_k}$ belongs to $H^q(\Omega_k)^2$, there exists a constant C such that:*

$$\begin{aligned}&\sup_{\boldsymbol{w}_h\in\boldsymbol{X}_h^\Omega} \frac{1}{\|\boldsymbol{w}_h\|_{\boldsymbol{X}_*^\Omega}} \textstyle\sum_{k=1}^K \langle \boldsymbol{w}_h^k\cdot\boldsymbol{t}, \operatorname{curl}\boldsymbol{e}\rangle_{\frac{1}{2},\partial\Omega_k} \\ &\qquad\le C\Big(\textstyle\sum_{k=1}^K h_k^q\big(\|\boldsymbol{e}^k\|_{H^q(\Omega_k)^2} + \|\operatorname{curl}\boldsymbol{e}^k\|_{H^q(\Omega_k)} + \|\boldsymbol{f}^k\|_{H^q(\Omega_k)^2}\big)\Big).\end{aligned}$$

Proof: Because of the regularity of $\boldsymbol{e}$ we write that

$$\begin{aligned}\sum_{k=1}^K \langle \boldsymbol{w}_h^k\cdot\boldsymbol{t}, \operatorname{curl}\boldsymbol{e}\rangle_{\frac{1}{2},\partial\Omega_k} &= \int_{\mathcal{S}} (\operatorname{curl}\boldsymbol{e})[\boldsymbol{w}_h\cdot\boldsymbol{t}] \\ &= \sum_{\Gamma_{k,i} \text{ not mortar}} \int_{\Gamma_{k,i}} (\operatorname{curl}\boldsymbol{e})(\boldsymbol{w}_h\cdot\boldsymbol{t} - \varphi_h)\ .\end{aligned}$$

Thanks to the matching constraints we deduce that, $\forall \psi_h \in W_h(\Gamma_{k,i})$,

$$\int_{\mathcal{S}} (\text{curl } \boldsymbol{e})[\boldsymbol{w}_h \cdot \boldsymbol{t}] \; = \sum_{\Gamma_{k,i} \text{ not mortar}} \int_{\Gamma_{k,i}} (\text{curl } \boldsymbol{e}^k - \psi_h)(\boldsymbol{w}_h \cdot \boldsymbol{t} - \varphi_h).$$

Choosing in particular ψ_h as being the continuous Lagrange interpolant in $W_h(\Gamma_{k,j}$ of (curl $\boldsymbol{e}^k$) over each non mortar $\Gamma_{k,i}$, we deduce that

$$\int_{\mathcal{S}} (\text{curl } \boldsymbol{e})[\boldsymbol{w}_h \cdot \boldsymbol{t}] \; = \sum_{\Gamma_{k,i} \text{ not mortar}} \|\text{curl } \boldsymbol{e}^k - \psi_h\|_{H_{00}^{\frac{1}{2}}(\Gamma_{k,i})} \|\boldsymbol{w}_h \cdot \boldsymbol{t} - \varphi_h\|_{H_{00}^{-\frac{1}{2}}(\Gamma_{k,i})}.$$

The end of the proof relies on the stability relation

$$\sum_{\Gamma_{k,i} \text{ not mortar}} \|\boldsymbol{w}_h \cdot \boldsymbol{t} - \varphi_h\|_{H_{00}^{-\frac{1}{2}}(\Gamma_{k,i})} \leq C \|\boldsymbol{w}_h\|_*,$$

and on the optimal error analysis concerning the interpolation operator. To recover a convergence rate of h^q using the finite element estimates (see [28]), it is necessary for (curl $\boldsymbol{e}^k$) to belong to $H^{q+1}(\Omega_k)$. This may be issued from equation (2.2) which yields that ∇(curl $\boldsymbol{e}^k$) is, actually, in $H^q(\Omega_k)^2$ provided that $\boldsymbol{e}^k$ and $\boldsymbol{f}^k$ belong to $H^q(\Omega_k)^2$. Due to the fact that curl $\boldsymbol{e}^k \in H^q(\Omega_k)$ it results that

$$\|\text{curl } \boldsymbol{e}^k\|_{H^{q+1}(\Omega_k)} \leq C\big(\|\boldsymbol{e}^k\|_{H^q(\Omega_k)^2} + \|\text{curl } \boldsymbol{e}^k\|_{H^q(\Omega_k)} + \|\boldsymbol{f}^k\|_{H^q(\Omega_k)^2}\big),$$

and this yields the consistency error estimate.□

Remark 4.2 *The hypothesis made on the regularity of the exact solution is not that stringent in practice. This situation may occur in many interesting physical situations. Think, for instance, to the magnetic field* $\boldsymbol{h}$ *and/or electric field* $\boldsymbol{e}$ *created in a non smooth domains. At the vicinity of the corners it presents a singular part which is the gradient of the singularities of the Poisson problem with the suitable boundary conditions. Hence the* curl *operator applied to* $\boldsymbol{e}$ *cancels the singularities and* curl $\boldsymbol{e}$ *is actually more regular than* $\boldsymbol{e}$.

4.3. *The final estimate*

Assembling the results of Lemma 4.7 and Theorem 4.6, via the Berger-Scott-Strang Lemma 4.1 we obtain the estimate of the global error made on the exact solution.

Theorem 4.8 *Let the exact solution* $\boldsymbol{e} \in \boldsymbol{X}^\Omega$ *be such that* $\boldsymbol{e}^k = \boldsymbol{e}_{|\Omega_k} \in H^q(\Omega_k)^2$ *and* curl $\boldsymbol{e}^k \in H^q(\Omega_k)$. *For data* $\boldsymbol{f}^k = \boldsymbol{f}_{|\Omega_k}$ *belonging to* $H^q(\Omega_k)^2$, *we have the following estimate*

$$\|\boldsymbol{e} - \boldsymbol{e}_h\|_{\boldsymbol{X}_*^\Omega} \leq C \sum_{k=1}^{K} h_k^q \big(\|\boldsymbol{e}^k\|_{H^q(\Omega_k)^2} + \|\text{curl } \boldsymbol{e}^k\|_{H^q(\Omega_k)} + \|\boldsymbol{f}^k\|_{H^q(\Omega_k)^2}\big). \quad (4.16)$$

5. Numerical discussion

In this section we present some numerical results that illustrates the numerical analysis performed before.

The computations are made on a squared domain $\Omega = (\frac{1}{2}, \frac{3}{2}) \times (\frac{1}{4}, \frac{3}{4})$ and we have used edge finite elements on triangular meshes (see [38]). More in detail, given the triangle κ, let $(\boldsymbol{x}_m)_{m=1,3}$ be its vertices and $\lambda_m(\boldsymbol{x})$ be the barycentric coordinate function associated to $\boldsymbol{x}_m$. To an edge $f_j^\kappa = (\boldsymbol{x}_m, \boldsymbol{x}_n)$, oriented from $\boldsymbol{x}_m$ to $\boldsymbol{x}_n$, is associated one vector function

$$\boldsymbol{w}_j(\boldsymbol{x}) = \lambda_m(\boldsymbol{x})\nabla\lambda_n(\boldsymbol{x}) \; - \; \lambda_n(\boldsymbol{x})\nabla\lambda_m(\boldsymbol{x}).$$

For any vector field vector $\boldsymbol{e} \in (\mathscr{C}(\overline{\kappa}))^3$ the interpolating function $\boldsymbol{e}_h$ on κ is provided by $\boldsymbol{e}_h = \alpha_j \boldsymbol{w}_j$, (the Einstein summation convention is used) with $\alpha_j(\boldsymbol{e}) = |f_j^\kappa|\,(\boldsymbol{e} \cdot \boldsymbol{t}_j^\kappa)(\boldsymbol{x}_m * \boldsymbol{x}_n)$, where $|f_j^\kappa|$ is the length of f_j^κ, $\boldsymbol{x}_m * \boldsymbol{x}_n$ its midpoint and $\boldsymbol{t}_j^\kappa$ its tangential unit vector. Then, in each κ the field $\boldsymbol{e}_h$ has the following form

$$\boldsymbol{e}_{h|\kappa}(\boldsymbol{x}) = \begin{pmatrix} a - cy \\ b + cx \end{pmatrix} \qquad a, b, c \in \mathbb{R}.$$

The computation of the curl of the shape functions is given by

$$\operatorname{curl} \boldsymbol{w}_j(\boldsymbol{x}) = 2\big(\partial_x\lambda_m(\boldsymbol{x})\partial_y\lambda_n(\boldsymbol{x}) - \partial_y\lambda_n(\boldsymbol{x})\partial_x\lambda_m(\boldsymbol{x})\big).$$

The analysis of the previous sections is readily extended to this reduced element that belongs to the first family of Nédélec edge elements in $H(\mathrm{curl})$.

First numerical example—. The goal is to approximate the solution of equation (2.2) in the domain Ω, with $\alpha = \beta = 1$ and $\boldsymbol{f}$ given in such a way that the exact solution is

$$\boldsymbol{e}(\boldsymbol{x}) = \begin{pmatrix} 2\pi \sin(\pi x)\cos(2\pi y) \\ -\pi \cos(\pi x)\sin(2\pi y) \end{pmatrix}.$$

A representation of the this field is provided in Figure 2.

We start by testing the conforming computations. For the structured meshes with different sizes (i.e., $h \in \{0.1, 0.05, 0.025, 0.0125\}$), we calculate the discrete solutions $\boldsymbol{e}_h$ and we plot in logarithmic scaling the convergence curves of the L^2-norm and the $H(\mathrm{curl}\,)$-norm of the gap between $\boldsymbol{e}_h$ and the interpolant of the exact solution $i_h\boldsymbol{e}$. Both errors are expected to decay with the same rate (because of the particular features of the interpolation operator i_h) since it can be easily stated from (2.7) and (3.11) that

$$\int_\Omega [\mathrm{curl}\,(\boldsymbol{e}_h - i_h\boldsymbol{e})]^2 \; d\boldsymbol{x} = \int_\Omega (\boldsymbol{e}_h - \boldsymbol{e})(\boldsymbol{e}_h - i_h\boldsymbol{e}) \; d\boldsymbol{x}.$$

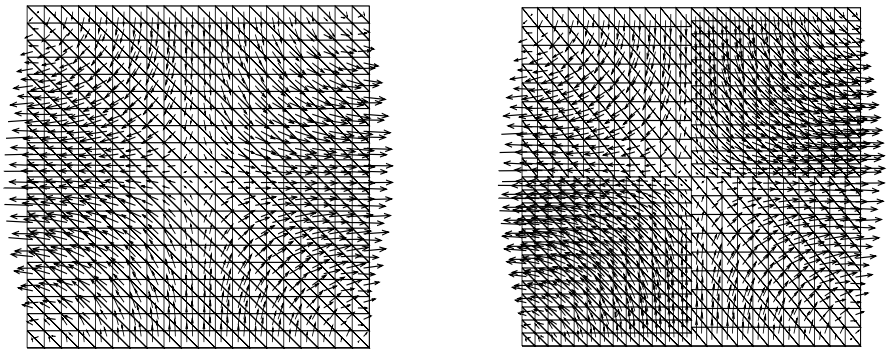

Figure 2: The interpolant $i_h \boldsymbol{e}$ of the exact vector field on a conforming mesh (left figure). The non-conforming mortar field is regular, no significant alteration is caused by the jumps along the interfaces (right figure).

The evaluation of the slopes of both curves concludes to a quadratic convergence of the computed solution with respect to both norms. The explanation of this super-convergence may be found in the conjunction of the particular nature of the exact solution ($\boldsymbol{e} = -\mathbf{curl}\,(\sin(\pi x)\sin(2\pi y))$ with the structured shape of the meshes.

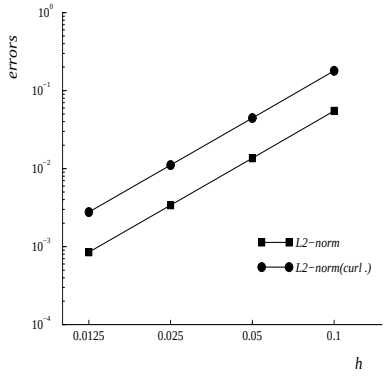

Figure 3: Convergence curves of the L^2-norm and the $H(\mathrm{curl})$-norm of the error $(\boldsymbol{e}_h - i_h \boldsymbol{e})$.

The domain Ω is then broken up into four squared sub-domains with the middle of Ω as a cross-point, as indicated in Figure 4 so as the choice of the mortar and non-mortar interfaces. The different meshes $(\mathscr{T}_h^k)_{1\leq k\leq 4}$ of the the sub-domains $(\Omega_k)_{1\leq k\leq 4}$ are taken structured and uniform. The numerical mortar finite element calculations are carried out using local triangular meshes of the sizes $\frac{4}{3}h$ in Ω_1 and Ω_4 and h in Ω_2 and Ω_3. For h in $\{0.1, 0.05, 0.025, 0.0125\}$, the errors $\|i_h\boldsymbol{e} - \boldsymbol{e}_h\|_{\boldsymbol{X}_*^\Omega}$ and $\|i_h\boldsymbol{e} - \boldsymbol{e}_h\|_{L^2(\Omega)^2}$ as functions of h are depicted in the Figure 5. We observe a

behavior which is similar to that for the conforming case, the approximated solution converges toward the exact one like $\mathcal{O}(h^2)$ in both spaces $L^2(\Omega)$ and $\boldsymbol{X}_*^{\Omega}$. The fact that the four sub-domains are discretized by triangular meshes that do not match at the skeleton of the decomposition does not affect or in a very little extent the electric field distribution. In fact, it can be remarked that the tangential component of the electric field seems to be transmitted from one domain to the neighboring ones without ostensible discontinuity.

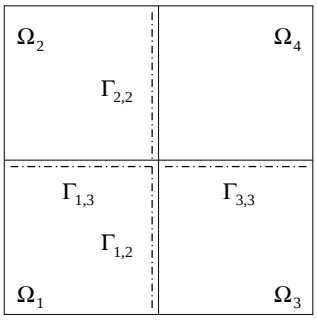

Figure 4: The decomposition of the domain Ω, the solid dark lines denote the masters and the dashed ones are the slaves.

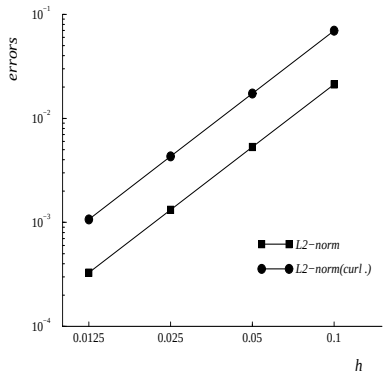

Figure 5: Quadratic convergence of the mortar Withney finite element solution, the slope of both curves is approximately 2.

Second numerical example—. The examination of the local accuracy along the mortar of the matching constraints is aimed by the second test. We consider the elementary electric field $\boldsymbol{e}^T(\boldsymbol{x}) = (1, 0)$ as the solution of problem (2.7). The data are then chosen so that $\boldsymbol{f} = \boldsymbol{e}$ and some Dirichlet conditions are enforced on the boundary, we have $\boldsymbol{e} \cdot \boldsymbol{t} = 1$ on the horizontal walls and $\boldsymbol{e} \cdot \boldsymbol{t} = 0$ on the vertical

walls. The discrete solution is calculated by the mortar approach using the domain decomposition chosen in the first example. We measure the gap between the tangential component along the mortars $\Gamma_{1,3}$ and $\Gamma_{3,3}$, of the interpolated field $i_h\boldsymbol{e}$ and the discrete solution $\boldsymbol{e}_h$ (i.e., $(i_h\boldsymbol{e} - \boldsymbol{e}_h)\cdot\boldsymbol{t}$)) and show in Figure 6 (in logarithmic scales) how its L^2-norm behaves with respect to the mesh size. Since the space $W_h(\Gamma_{1,3}\cup\Gamma_{3,3})$ of tangential traces of the discrete fields involves all the piece-wise constant functions it is expected that the convergence rate is of order $\mathcal{O}(h)$ which is confirmed by the slope of the linear regression of the error curve ≈ 0.997.

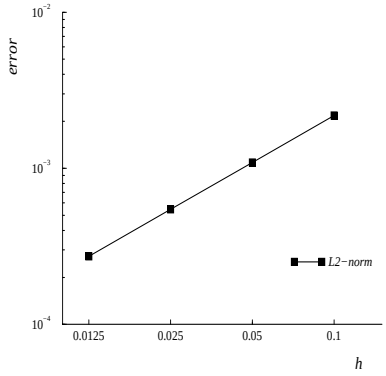

Figure 6: Linear convergence of the error $((i_h\boldsymbol{e}-\boldsymbol{e}_h)\cdot\boldsymbol{t})$ along the horizontal mortars.

6. Concluding Remarks

This work, the substantial part of which was achieved in 1997, is the first contribution in the extension of the mortar finite element method of class $H(\text{curl})$ in view of handling electromagnetic models governed by the full Maxwell equations. This technique is studied and implemented in [27,40] for the computation of the eddy-currents in moving structures (like a rotor/stator device) using sliding meshes. The generalization to the three dimensions turns to be technically more difficult and is addressed successfully in [13,26] for the numerrical analysis and we refer to [22,23] for some attractive applications.

References

1. Y. Achdou and Yu. A. Kuznetsov, *Substructuring Preconditioners for Finite Element Methods on Nonmatching Grids*, *East–West J. Numer. Math.*, **3** (1995) 1–28.
2. Y. Achdou, Y. Maday and O. B. Widlund, *Iterative Substructuring Preconditioners for the Mortar Finite Element Method in Two Dimensions*, *SIAM J. Num. Anal.*, **36** (1999) 551–580.
3. Y. Achdou and O. Pironneau, *A Fast Solver for Navier-Stokes Equations in the Laminar Regime Using Mortar Finite Element and Boundary Element Methods*, *SIAM J. Num.*

Anal., **32** (1995) 985–1016.
4. R. Adams, **Sobolev Spaces**, (Academic press, 1975).
5. A. Agouzal and J.-M. Thomas, *Une méthode d'éléments finis hybride en décomposition de domaines*, *Modél. Math. et Anal. Numér.*, **29** (1995) 749–764.
6. G. Anagnostou, *Non Conforming Sliding Spectral Element Methods for Unsteady Incompressible Navier-Stokes Equations*, *Ph. D. Thesis, Massachusetts Institute of Technology, Cambridge* (1991).
7. F. Assous, P. Degond and J. Segré, *Numerical Approximation of The Maxwell Equations in Inhomogeneous Media by a $\mathbb{P}_1$ conforming Finite Element Method*, *J. Comput. Phys.*, **128** (1996) 363–380.
8. Z. Belhachmi, *Méthodes d'éléments spectraux avec joints pour la résolution de problèmes d'ordre quatre*, *Thesis, Université Pierre et Marie Curie, Paris* (1994).
9. F. Ben Belgacem, *The Mortar Finite Element Method with Lagrange Multipliers*, *Numer. Math.* (2002) to appear.
10. F. Ben Belgacem, *Discrétisations 3D non conformes par la méthode de décomposition de domaine des éléments avec joints : Analyse mathématique et mise en œuvre pour le problème de Poisson*, *Thesis, Université Pierre et Marie Curie, Paris* (1993).
11. F. Ben Belgacem, *The mixed mortar finite element method for the incompressible Stokes problem: convergence analysis. SIAM J. Numer. Anal.*, **37** (2000) 1085–1100.
12. F. Ben Belgacem, C. Bernardi, N. Chorfi , Y. Maday. *Inf-sup conditions for the mortar spectral element discretization of the Stokes problem. Numer. Math.*, **85** (2000) 257–281.
13. F. Ben Belgacem, A. Buffa and Y. Maday, *The Mortar Finite Element Method for 3D Maxwell Equations: First Results*, SIAM J. Num. Anal. **39** (2001) 880–901.
14. F. Ben Belgacem, P. Hild and P. Laborde, *Extension of the Mortar Finite Element Method to a Variational Inequality Modeling Unilateral Contact*, *Mathematical Models and Methods in Applied Sciences* **9** (1999) 287–303.
15. F. Ben Belgacem and Y. Maday, *Non Conforming Spectral Element Methodology Tuned to Parallel Implementation*, *Compu. Meth. Appl. Mech. Eng.* **116** (1994) 59-67.
16. A. Berger, R. Scott and G. Strang, *Approximate Boundary Conditions in the Finite Element Method*, *Symposia Mathematica* **10** (1972) 295–313.
17. C. Bernardi and V. Girault, *A Local Regularisation Operator for Triangular and Quadrangular Finite Elements*, *SIAM J. Num. Anal.* **35** (1998) 1893–1916.
18. C. Bernardi, F. Hecht. *Error indicators for the mortar finite element discretization of the Laplace equation. Math. Comp.*, **71** (2002) 1371–1403.
19. C. Bernardi, Y. Maday and A. T. Patera, *A New Non Conforming Approach to Domain Decomposition: The Mortar Element Method*, in *Nonlinear partial differential equations and their applications*, eds. H. Brezis and J.-L. Lions (Pitman, 1994) 13–51.
20. S. Bertoluzza and V. Perrier, *The mortar element method in the wavelet context*, *Méth. Math. en Anal. Num.* **35** (2001) 647–673.
21. F. Bouillault, A. Buffa, Y. Maday, F. Rapetti. *Simulation of a magneto-mechanical damping machine: analysis, discretization, results. Comput. Methods Appl. Mech. Engrg.*, **191** (2002) 2587–2610.
22. F. Bouillault, A. Buffa, Y. Maday, F. Rapetti. *The mortar edge element method in three dimensions: application to magnetostatics*, *SIAM J. on Scient. Comp.*, **24 (4)** (2002) 1303–1327.
23. F. Rapetti, F. Bouillault, Y. Maday, A. Razek. *Eddy current calculations in three-dimensional moving structures*, *IEEE Transactions on Magnetics*, **38 (2)** (2002) 613–616.
24. D. Braess, W. Dahmen and C. Wieners, *A Multigrid Algorithm for Mortar Element Method*, *SIAM J. Num. Anal.*, **37** (1999) 48–69.

25. F. Brezzi and D. Marini. *Error Estimates for the Three-field Formulation with Bubble Stabilization. Math. Comp.*, **70** (2001) 911–934.
26. A. Buffa. *Some numerical and theorerical problems in computational electromagnetics. Ph. D. Thesis, the Università di Pavia*, Pavia (2000).
27. A. Buffa, Y. Maday and F. Rapetti, *A sliding mesh-mortar method for a two dimensional eddy currents model of electric engines*, *Méth. Math. en Anal. Num.* **35 (2)** (2001) 191–228.
28. P.-G. Ciarlet, **The Finite Element Method for Elliptic Problems**, (North Holland, Amsterdam 1978).
29. R. Dautray and J.-L. Lions, **Analyse mathématique et calcul numérique pour les sciences et les techniques 2** (Masson, 1987).
30. N. Débit, *La méthode des éléments avec joints dans le cas du couplage des méthodes spectrales et d'éléments finis: Résolution des équations de Navier-Stokes*, *Thesis, Université Pierre et Marie Curie, Paris* (1992).
31. P. Fernandes and M. Raffetto. *The question of spurious modes revisited*, *ICS Newsletter*, **7 (1)** (2000) 5–8.
32. V. Girault and P.-A. Raviart, **Finite Element Methods for Navier-Stokes Equations** (Springer Verlag, 1986).
33. P. Grisvard, *Elliptic Problems in Nonsmooth Domains*, *Monographs and Studies in Mathematics* **24** (Pitman, 1985).
34. P. Hild. **Problèmes de contact unilatéral et maillages incompatibles**, *Thèse de l'Université Paul Sabatier, Toulouse* (1998).
35. J. Jin, **The Finite Element Method in Electromagnetics** (Wiley, New York 1993).
36. R. Krause, B. Wohlmuth. Nonconforming domain decomposition techniques for linear elasticity, *East-West J. Numer. Anal.* **8** (2000) 177–206.
37. P. Le Tallec and T. Sassi, *Domain Decomposition Algorithms with Nonmatching Grids*, *Math. of Compu.* **64** (1995) 1367–1396.
38. J.-C. Nédélec, *Mixed Finite Element in* $\mathbb{R}^3$, *Numer. Math.*, **35** (1980) 315–341.
39. J.-C. Nédélec, *New Family of Mixed Finite Element in* $\mathbb{R}^3$, *Numer. Math.*, **50** (1986) 57–81.
40. F. Rapetti. *Approximation des équations de la magnétodynamique en domaine tournant par la méthode des éléments avec joints. Thesis, Université Pierre et Marie Curie, Paris* (2000).
41. A. Toselli, *Domain Decomposition Methods for Vector Field Problems*, *Ph. D. Thesis, Courant Institute of Mathematical Sciences, New York* (1999).
42. B. I. Wohlmuth, *A Residual Based Error Estimator for Mortar Finite Discretization*, *Numer. Math.*, **84** (1999) 143–171.